Supplementary Information

Unexpected molecular diversity of brown carbon formed by Maillard-like reactions in aqueous aerosols

Shanshan Tang[a,b], Feifei Li[b,f], Jitao Lv*[,b,f], Lei Liu[c,d], Guangming Wu[e,f], Yarui Wang[b,f], Wanchao Yu[b,f], Yawei Wang*[,a,b,f], Guibin Jiang[a,b,f]

[a]School of Environment, Hangzhou Institute for Advanced Study, University of Chinese Academy of Sciences, Hangzhou 310024, China

[b]State Key Laboratory of Environmental Chemistry and Eco-toxicology, Research Center for Eco-environmental Sciences, Chinese Academy of Sciences, Beijing 100085, China

[c]Department of Atmospheric Sciences, School of Earth Sciences, Zhejiang University, Hangzhou 310027, China

[d]Beihang Hangzhou Innovation Institute Yuhang, Hangzhou 310023, China

[e]Key Laboratory of Tibetan Environment Changes and Land Surface Processes, Institute of Tibetan Plateau Research, Chinese Academy of Sciences, Beijing 100101, China

[f]University of Chinese Academy of Sciences, Beijing 100049, China

*E-mail: ywwang@rcees.ac.cn, jtlv@rcees.ac.cn

Text S1. Desalination of products

The desalination of resulting colored products was performed by solid-phase extraction (SPE) using Bond Elute PPL cartridges (1 g per 6 mL; Varian, Palo Alto, CA). Briefly, the cartridges were rinsed with 6 mL of methanol (MS grade) and pure water respectively prior to use. The solution after the reaction was acidified to pH 2 with HCl (32%, ultrapure), and then passed through the cartridges by gravity at a flow rate of approximately 2 mL min^{-1}. Cartridges were rinsed with three volumes of 0.01 M HCl for the removal of salts, dried with a pump and immediately extracted with three volumes of methanol (MS grade). Eluted samples were concentrated in the rotary evaporator at 45°C, and then blow-dried with N_2. The extraction efficiencies of reactants by PPL-based SPE were about zero according to their TOC recoveries, thus the remaining samples after solid-phase extraction do not include reactants. The dried samples were stored in 2 mL brown vial and weighted to estimate the particle yield using the following formula (Eqn. S1):

$$\text{Yield (\%)} = \frac{\text{mass}_{\text{dried-product}}}{\text{mass}_{\text{organic-reactant}}} \times 100\% \qquad \text{(S1)}$$

Text S2. UV–Vis and Fluorescence experiments

In an effort to explore the endpoint of the reaction and assess the rate of BrC formation, UV−Vis absorption spectra of each reaction mixture were acquired at regular intervals from the beginning of the reaction. The samples for all investigated reaction systems were diluted 300 times with ultrapure water at different time points. The ultrapure water was used as reference. The optical properties of BrC samples were quantified by calculating the mass absorption efficiency at 365 nm (MAE_{365}, m^2/g C) and absorption Ångström exponent (AAE) in the UV (250−400 nm) and near-vis (400−480 nm) ranges using the following equation[1,2]:

$$\mathrm{MAE}_{365} = \frac{(A_{365} - A_{700}) \times \ln(10)}{C_{\mathrm{mass}} \times l} \quad \text{(S2)}$$

$$\mathrm{AAE} = \frac{-\ln\left(\frac{\mathrm{MAE}_{\lambda_1}}{\mathrm{MAE}_{\lambda_2}}\right)}{\ln\left(\frac{\lambda_1}{\lambda_2}\right)} \quad \text{(S3)}$$

Where A_{365} and A_{700} are the absorbances in UV–Vis measurements, C_{mass} is the TOC concentration measured in g m^{-3}, and l is the path length (1 cm). Because of weak absorption at wavelength 365 nm from other nonorganic compounds[3], thus the MAE_{365} was taken as the surrogate for BrC in this study. It should be noted that the samples were kept in dark conditions before absorbance and TOC measurements.

The emission and excitation wavelengths of the fluorescence spectra were from 250 to 600 nm and 230 to 550 nm, respectively. The wavelength increments of the emission and excitation scans were 2 and 5 nm, respectively. The fluorescence calibration is mainly modified by the previous studies[4,5]. It includes instrumental bias correction, inner filter effect correction, Raman calibration and blank subtraction. Generally, the instrumental bias correction offered by the instrument's manufacturer is automatically applied to adjust the raw fluorescence data, which are finally reported in the Sc/Rc (corrected signal/corrected reference) model. Secondly, the inner filter effect (IFE) could result in the fluorescence underestimation[4,6], which employed the following common method:

$$F^{IFE} = F^{ori} \times 10^{0.5 \cdot (A_{\lambda ex} + A_{\lambda em})} \quad \text{(S4)}$$

where F^{IFE} and F^{ori} represent the IFE corrected and original fluorescence data obtained from the spectrophotometer, respectively. The value of 0.5 is the half of optical path length of the cuvette (usually is 1 cm). The parameters $A_{\lambda ex}$ and $A_{\lambda em}$ correspond to the absorbances of excitation and emission light at a certain wavelength (λ). Thirdly, all the fluorescence data for samples and blanks

are normalized to the Raman data collected on the same day, and then reported the corrected fluorescence data (F^{Raman}) in Raman Units (RU). For BrC samples in this study, the IFE corrected fluorescence data (F^{IFE}) was calibrated by the Raman peak area (A_{rp}^{350}), which was derived from the integrated water Raman ($WR_{350,\lambda em}$) between wavelengths 381 and 426 nm at the excitation wavelength of 350 nm:

$$F^{Raman} = \frac{1}{A_{rp}^{350}} \times F^{IFE} \quad \text{(S5)}$$

$$A_{rp}^{350} = \int_{381}^{426} WR_{350,\lambda_{em}} d\lambda_{em} \quad \text{(S6)}$$

The Raman signals of water are not constant due to various factors, such as light source fluctuation. Therefore, the Raman data were collected daily. Finally, the fluorescence data for each sample further subtracted the blank sample.

The fluorescence index (FI), biological index (BIX) and humidification index (HIX) parameters calculated by the fluorescence intensity (F) ratios between certain excitation/emission wavelength ranges have been shown to be practical metrics to provide specific source information of atmospheric aerosols[7].

$$\text{FI} = \frac{F(Ex = 370\ nm, Em = 450\ nm)}{F(Ex = 370\ nm, Em = 500\ nm)} \quad \text{(S7)}$$

$$\text{BIX} = \frac{F(Ex = 310\ nm, Em = 380\ nm)}{F(Ex = 310\ nm, Em = 430\ nm)} \quad \text{(S8)}$$

$$\text{HIX} = \frac{F(Ex = 255\ nm, Em = 434 - 480\ nm)}{F(Ex = 255\ nm, Em = 300 - 345\ nm)} \quad \text{(S9)}$$

In addition, the Parallel Factor Analysis (PARAFAC) was tried for the BrC samples in this study, but it failed. Meanwhile, Pitta and Zeri proposed that the inappropriate performance of PARAFAC on datasets originating from various sources is likely to occur[8].

Text S3. Ultrahigh-Resolution ESI FT−ICR MS Analysis

The instrument parameters for the analysis can be found in the previous publications[9,10]. Briefly, ultrahigh-resolution mass spectra of all the samples were acquired in both −ESI and +ESI sources with broadband detection, and three replicates of each sample were examined. A much higher molecular diversity of secondary BrC can be obtained by combining the two modes than by either −ESI or +ESI mode. Moreover, N-containing molecules were readily protonated in +ESI mode[11], which accounted for 55% and 45% of the +ESI-unique formulas and −ESI-unique formulas, respectively. Samples were continuously infused into the ESI unit by syringe infusion at a flow rate of 120 μL h^{-1}, and the ESI needle voltage was set to −3.8 kV and 4.0 kV in −ESI and +ESI mode, respectively. The lower and upper mass limit was set to a mass-to-charge ratio (m/z) of 120 and 928, respectively. Ions were accumulated in a hexapole ion trap for 0.06 sec before being introduced into the ICR cell. 4M words of data were recorded per broadband mass scan. A total of 200 scans were summed for each mass spectrum. The spectra were externally calibrated with 10 mM of sodium formate solution in 50% isopropyl alcohol using a linear calibration and then internally recalibrated with an in-house reference mass list. After internal calibration, the mass error was < 500 ppb over the entire mass range. Peaks were identified with Bruker Data Analysis software. For each ionization mode, the normalization signal intensities were used. Regarding the shared formula in −ESI and +ESI sources, CHO and CHOS formulas were used the normalization signal intensities obtained by −ESI mode, while CHON and CHONS formulas were used the normalization signal intensities obtained by +ESI mode.

Text S4. Molecular Parameters

With some criteria, 3 and 2 formulas were identified by −ESI and +ESI mode, respectively, in the blank control, and these formulas were excluded if they were detected in the BrC samples. The O/C

as the abscissa and the H/C as the ordinate were used to construct the Van Krevelen diagram[12]. The following parameters for data analysis were calculated: double bond equivalents (DBE) as a measurement of the number of double bonds and rings in a molecule[13], modified aromaticity index proposed by Koch and Dittmar as a measurement of the extent of aromatic and condensed aromatic structures (AI_{mod})[14], and the average carbon oxidation state ($\bar{OSc}$)[15]. From the molecular formula ($C_cH_hO_oN_nS_s$) assignments, DBE and AImod can be expressed as:

$$DBE = 1 + (2c - h + n)/2 \quad \text{(S10)}$$

$$AI_{mod} = (1 + c - \frac{o}{2} - \frac{h}{2})/(c - \frac{o}{2} - n) \quad \text{(S11)}$$

$$\overline{OS_C} \approx 2O/C - H/C \quad \text{(S12)}$$

where *c*, *h*, *n* and *o* refer to the stoichiometric numbers of carbon, hydrogen, nitrogen and oxygen atoms per formula. The magnitude averaged C, H, O, N and O/C, H/C, DBE, AImod and $\bar{OSc}$ values for each BrC sample were calculated according to the previous studies[9,11] and can be determined by the following formula:

$$(M)_w = \left(\sum_i I_i \times (M)_i\right) / \sum_i I_i \quad \text{(S13)}$$

where *M* represents parameters C, H, O, N and O/C, H/C, DBE, AImod and $\bar{OSc}$ respectively, *w* signifies a magnitude-averaged calculation. I_i and $(M)_i$ are the relative abundance and M value of peak *i*, respectively. The relative abundance is calculated as the abundance of the individual peak divided by the maximum of abundances in a given spectrum.

Notes and references

1. N. Y. Kasthuriarachchi, L.-H. Rivellini, X. Chen, Y. J. Li and A. K. Y. Lee, *Environ. Sci. Technol.*, 2020, **54**, 13207-13216.
2. A. Laskin, J. Laskin and S. A. Nizkorodov, *Chem. Rev.*, 2015, **115**, 4335-4382.
3. G. Wu, K. Ram, P. Fu, W. Wang, Y. Zhang, X. Liu, E. A. Stone, B. B. Pradhan, P. M.

Dangol, A. K. Panday, X. Wan, Z. Bai, S. Kang, Q. Zhang and Z. Cong, *Environ. Sci. Technol.*, 2019, **53**, 3471-3479.
4. K. R. Murphy, K. D. Butler, R. G. M. Spencer, C. A. Stedmon, J. R. Boehme and G. R. Aiken, *Environmental Science & Technology*, 2010, **44**, 9405-9412.
5. P. Fu, K. Kawamura, J. Chen, M. Qin, L. Ren, Y. Sun, Z. Wang, L. A. Barrie, E. Tachibana and A. Ding, *Scientific reports*, 2015, **5**, 9845.
6. D. N. Kothawala, K. R. Murphy, C. A. Stedmon, G. A. Weyhenmeyer and L. J. Tranvik, *Limnology and Oceanography-Methods*, 2013, **11**, 616-630.
7. G. Wu, P. Fu, K. Ram, J. Song, Q. Chen, K. Kawamura, X. Wan, S. Kang, X. Wang, A. Laskin and Z. Cong, *Environ. Pollut.*, 2021, **268**, 115906.
8. E. Pitta and C. Zeri, *Spectrochim. Acta A*, 2021, **258**, 119800.
9. J. Lv, R. Han, Z. Huang, L. Luo, D. Cao and S. Zhang, *ACS Earth Space Chem.*, 2018, **2**, 330-339.
10. D. Cao, J. Lv, F. Geng, Z. Rao, H. Niu, Y. Shi, Y. Cai and Y. Kang, *Anal. Chem.*, 2016, **88**, 12210-12218.
11. Y. Miao, J. Lv, H. Huang, D. Cao and S. Zhang, *J. Environ. Sci.*, 2020, **98**, 22-30.
12. T. Reemtsma, *Journal of Chromatography A*, 2009, **1216**, 3687-3701.
13. J. Lv, S. Zhang, S. Wang, L. Luo, D. Cao and P. Christie, *Environmental Science & Technology*, 2016, **50**, 2328-2336.
14. B. P. Koch and T. Dittmar, *Rapid Commun. Mass Spectrom.*, 2006, **20**, 926-932.
15. J. H. Kroll, N. M. Donahue, J. L. Jimenez, S. H. Kessler, M. R. Canagaratna, K. R. Wilson, K. E. Altieri, L. R. Mazzoleni, A. S. Wozniak, H. Bluhm, E. R. Mysak, J. D. Smith, C. E. Kolb and D. R. Worsnop, *Nat. Chem.*, 2011, **3**, 133-139.
16. L. Liu, J. Zhang, Y. Zhang, Y. Wang, L. Xu, Q. Yuan, D. Liu, Y. Sun, P. Fu, Z. Shi and W. Li, *Atmos. Chem. Phys.*, 2021, **21**, 2251-2265.
17. C. J. Kampf, A. Filippi, C. Zuth, T. Hoffmann and T. Opatz, *Phys. Chem. Chem. Phys.*, 2016, **18**, 18353-18364.

Table S1. Detailed information on $PM_{2.5}$ samples collected at the rural (Baoding) and urban (Jinan) sites[16].

Location	Date	Local time	Sampling duration (h)	$PM_{2.5}$ ($\mu g/m^3$)	$[NH_4^+]$ ($\mu g/m^3$)	Number of formulas	Number of shared formulas	Number of CHON	Number of shared CHON
Rural	12 Nov. 2016	8:30	10.9	153.22	9.953	1346	689	240	195
	12 Nov. 2016	20:50	11.5	271.15	13.586	894	408	120	96
	13 Nov. 2016	8:40	11.5	263.68	19.267	2462	944	429	312
	14 Nov. 2016	8:50	11.5	208.08	16.950	1842	729	288	207
	14 Nov. 2016	20:30	11.5	153.42	5.931	828	367	157	126
	15 Nov. 2016	22:00	11.5	256.12	10.789	1880	876	591	412
	16 Nov. 2016	20:30	11.5	266.56	14.610	1618	781	387	299
Urban	13 Nov. 2016	20:24	11.5	182.522	18.117	2138	1044	432	350
	14 Nov. 2016	20:30	11.5	181.377	21.318	631	315	33	26
	14 Nov. 2016	20:24	11.5	68.724	3.650	412	264	106	70

Table S2. The used chemical transformations in this study.

System	Label	Mass difference	Elements	Number
AS−MG	**MG**	72.021129	$C_3H_4O_2$	1511
	A	51.010899	C_3HN	1079
Gly−MG	**MG**	72.021129	$C_3H_4O_2$	2982
	Gly	75.032028	$C_2H_5O_2N$	1718

Table S3. The mass yield and optical parameters of secondary brown carbon products after solid phase extraction (PPL).

Sample	Y (%)	$SUVA_{254}$	MAE_{365}	$AAE_{300\text{-}400}$	FI	BIX	HIX
AS−HA	0.22	1.04	0.15	13.25	1.32	0.67	2.20
AS−GX	0.03	3.10	4.50	3.33	0.89	0.95	1.27
AS−MG	1.93	1.97	0.59	7.47	1.26	0.69	6.40
AS−AC	21.43	0.80	0.37	5.07	1.17	1.07	1.79
AS−GAld	6.83	1.28	2.45	3.72	1.01	0.63	20.58
Gly−HA	0.09	2.10	1.31	5.86	1.17	0.78	4.82
Gly−GX	1.82	2.60	3.42	3.72	1.42	0.27	17.24
Gly−MG	6.33	1.66	2.64	4.53	1.08	0.47	21.42
Gly−AC	7.86	1.46	0.35	6.71	1.57	0.93	1.23
Gly−GAld	7.63	1.15	2.47	4.04	1.12	0.59	30.04
EA−MG	18.96	3.29	3.95	3.93	1.10	0.25	26.23
PA−MG	17.33	2.76	3.52	4.08	1.03	0.24	23.73

Table S4. Average relative contributions of total spectral intensity for integrations of major proton regions in ^1H NMR spectra for secondary brown carbon products after solid-phase extraction (PPL).

Sample	H−C (0.6–1.8 ppm)	H−C−C= (1.8–3.2 ppm)	H−C−O−R (3.2–4.4 ppm)	Ar−H (6.0–9.0 ppm)
AS−HA	42.49	24.09	28.38	5.04
AS−GX	13.33	5.71	74.55	6.41
AS−MG	46.76	34.57	14.92	3.75
AS−AC	20.82	34.76	43.09	1.33
AS−GAld	3.50	23.48	61.74	11.29
Gly−HA	42.30	19.49	34.79	3.43
Gly−GX	0.02	7.67	92.22	0.09
Gly−MG	34.69	39.98	24.90	0.43
Gly−AC	16.26	33.78	41.62	8.34
Gly−GAld	5.17	28.71	64.66	1.46
EA−MG	52.14	20.10	24.66	3.10
PA−MG	57.05	21.38	17.89	3.68

Table S5. The number of assigned formulas in −ESI and +ESI (total), the average empirical formulas and molecular characteristics for secondary brown carbon products identified by −ESI and +ESI, w signifies a magnitude-weighted calculation.

Sample	Category	Total	C_w	H_w	N_w	O_w	MW_W	H/C_w	O/C_w	DBE_w	$AI_{mod,w}$	$\bar{O}Sc$	CHO (%)	CHON (%)
AS−HA	−ESI	1313	18.01	24.93	0.18	8.06	379.64	1.41	0.48	6.63	0.10	-0.46	49.05	32.29
	+ESI	3010	22.47	31.12	0.63	7.43	432.50	1.40	0.34	7.90	0.21	-0.72	23.92	63.16
AS−GX	−ESI	898	14.49	18.49	0.82	7.52	331.30	1.26	0.55	6.66	0.24	-0.17	36.19	53.90
	+ESI	1415	16.51	21.05	1.48	6.76	360.36	1.32	0.43	7.93	0.24	-0.50	11.02	61.09
AS−MG	−ESI	1618	17.43	21.91	0.67	9.52	393.83	1.27	0.56	7.44	0.19	-0.15	31.21	59.95
	+ESI	1296	21.01	26.58	1.42	8.56	440.11	1.28	0.42	9.14	0.26	-0.44	9.72	68.75
AS−AC	−ESI	327	16.73	24.71	0.52	5.84	333.40	1.55	0.39	5.64	0.04	-0.77	50.46	36.09
	+ESI	447	21.00	33.57	1.66	6.25	411.01	1.61	0.30	5.60	0.12	-1.00	3.13	83.45
AS−Gald	−ESI	691	17.02	23.38	1.48	8.64	389.29	1.32	0.52	6.80	0.13	-0.29	3.62	87.70
	+ESI	1388	20.37	27.43	2.26	9.25	446.56	1.35	0.46	8.31	0.22	-0.44	0.14	97.26
Gly−HA	−ESI	683	16.19	21.26	1.55	6.92	347.05	1.33	0.44	6.84	0.26	-0.44	13.32	86.68
	+ESI	2745	20.85	27.28	1.77	7.96	430.69	1.32	0.39	8.59	0.27	-0.54	11.62	88.38
Gly−GX	−ESI	398	17.60	24.07	0.61	14.39	473.11	1.34	0.89	6.37	0.31	0.34	40.45	59.55
	+ESI	351	21.22	22.88	2.11	10.00	468.29	1.12	0.52	11.34	0.30	-0.08	5.98	94.02
Gly−MG	−ESI	1463	19.05	22.89	1.60	9.65	427.30	1.20	0.51	8.90	0.30	-0.19	10.73	89.27
	+ESI	2217	20.33	24.97	1.85	9.69	451.01	1.23	0.48	9.27	0.30	-0.27	5.95	94.05
Gly−AC	−ESI	368	19.61	27.27	2.02	6.88	400.09	1.39	0.35	7.49	0.25	-0.69	0.54	99.46
	+ESI	1157	21.89	31.04	1.95	7.68	440.54	1.43	0.35	7.85	0.21	-0.72	0.61	99.39
Gly−Gald	−ESI	340	13.86	18.44	1.31	8.10	331.84	1.34	0.59	5.80	0.17	-0.16	7.06	92.94
	+ESI	1649	19.49	25.40	2.16	10.21	454.04	1.31	0.53	8.37	0.21	-0.25	0.91	99.09
EA−MG	−ESI	1130	18.29	25.55	2.29	5.35	362.04	1.35	0.30	7.17	0.27	-0.75	2.04	97.96
	+ESI	959	19.28	27.29	2.78	3.52	354.98	1.43	0.18	7.52	0.32	-1.07	1.15	98.85
PA−MG	−ESI	928	17.54	26.53	2.04	5.33	350.18	1.53	0.32	5.80	0.18	-0.89	3.56	96.44
	+ESI	1196	19.15	30.50	2.76	2.41	338.80	1.63	0.12	5.79	0.23	-1.39	0.59	99.41

Table S6. The number of assigned formulas, the average empirical formulas and molecular characteristics for one set of secondary brown carbon products combined −ESI and +ESI, w signifies a magnitude-weighted calculation.

Sample	Total	C_w	H_w	N_w	O_w	MW_W	H/C_w	O/C_w	DBE_w	$AI_{mod,w}$	$\bar{O}Sc_w$	O/N (%)	CHO (%)	CHON (%)
AS−HA	4323	20.87	28.89	0.47	7.66	413.50	1.40	0.39	7.44	0.17	-0.63	93.81	31.55	53.78
AS−GX	2313	15.38	19.61	1.10	7.19	344.02	1.29	0.50	7.21	0.24	-0.30	83.78	20.80	58.32
AS−MG	2914	19.22	24.24	1.05	9.04	416.97	1.28	0.49	8.29	0.23	-0.29	92.91	21.65	63.86
AS−AC	774	18.32	28.00	0.95	5.99	362.26	1.57	0.36	5.62	0.07	-0.86	86.18	23.13	63.44
AS−GAld	2079	19.13	25.93	1.97	9.02	425.38	1.34	0.48	7.75	0.19	-0.39	92.44	1.30	94.08
Gly−HA	3428	20.33	26.62	1.74	7.84	421.48	1.32	0.40	8.40	0.27	-0.53	94.40	11.96	88.01
Gly−GX	749	19.20	23.54	1.27	12.45	470.98	1.24	0.70	8.57	0.31	-0.15	99.47	24.30	75.70
Gly−MG	3680	19.59	23.77	1.71	9.66	437.36	1.21	0.50	9.06	0.30	-0.22	95.25	7.85	92.15
Gly−AC	1525	21.09	29.71	1.97	7.40	426.25	1.42	0.35	7.72	0.22	-0.71	94.26	0.59	99.41
Gly−GAld	1989	18.89	24.66	2.07	9.99	441.15	1.31	0.54	8.10	0.20	-0.24	96.82	1.96	98.04
EA−MG	2089	18.51	25.93	2.40	4.96	360.51	1.37	0.28	7.24	0.28	-0.82	48.10	1.63	98.37
PA−MG	2124	17.95	27.52	2.22	4.60	347.34	1.55	0.27	5.80	0.20	-1.02	45.00	1.88	98.12

Table S7. The number of assigned formulas, the average empirical formulas and molecular characteristics for one set of secondary brown carbon products combined −ESI and +ESI, a signifies an average calculation.

Sample	Total	C_a	H_a	N_a	O_a	MW_a	H/C_a	O/C_a	DBE_a	$AI_{mod,a}$	$\bar{O}Sc_a$
AS−HA	4323	22.55	31.43	0.73	7.62	439.17	1.40	0.36	8.19	0.19	-0.68
AS−GX	2313	16.53	19.57	1.22	8.21	373.25	1.18	0.52	8.39	0.30	-0.14
AS−MG	2914	20.82	25.19	1.13	8.96	438.99	1.23	0.45	9.53	0.27	-0.33
AS−AC	774	20.31	30.79	1.13	6.32	396.07	1.52	0.33	6.33	0.14	-0.85
AS−GAld	2079	20.13	27.17	2.01	9.24	434.39	1.33	0.47	8.33	0.20	-0.39
Gly−HA	3428	21.92	28.67	1.65	8.05	443.68	1.29	0.38	9.21	0.29	-0.54
Gly−GX	749	20.97	23.91	1.51	12.05	489.75	1.16	0.62	10.24	0.18	0.07
Gly−MG	3680	20.55	25.21	1.73	9.53	448.66	1.22	0.47	9.41	0.30	-0.29
Gly−AC	1525	22.89	32.76	1.97	7.67	453.13	1.42	0.34	8.26	0.22	-0.74
Gly−GAld	1989	19.80	25.96	1.98	9.75	447.57	1.29	0.50	8.64	0.24	-0.29
EA−MG	2089	20.02	27.18	2.32	5.17	382.82	1.35	0.27	8.05	0.30	-0.81
PA−MG	2124	21.09	31.01	2.28	4.79	392.97	1.49	0.24	7.29	0.23	-1.00

Table S8. The relative content (%) of the four classification groups for the assigned formulas (Group 1: condensed polycyclic aromatics; Group 2: polyphenols; Group 3: highly unsaturated and phenolic compounds; Group 4: aliphatic compounds).

Sample	Group 1	Group 2	Group 3	Group 4
AS−HA	0.02	2.30	67.88	29.80
AS−GX	7.62	15.81	64.17	12.40
AS−MG	0.34	9.79	80.60	9.27
AS−AC	1.19	0.53	46.68	51.59
AS−GAld	0.19	6.77	74.96	18.08
Gly−HA	0.03	2.33	88.62	9.01
Gly−GX	8.95	17.76	61.42	11.88
Gly−MG	0.24	10.96	82.14	6.66
Gly−AC	0.00	0.92	72.81	26.27
Gly−GAld	0.15	8.61	77.05	14.19
EA−MG	0.00	5.73	72.94	21.33
PA−MG	0.00	0.34	59.13	40.54

Table S9. MS/MS fragment ions in AS−MG and Gly−MG.

System	Form	Observed mass	Standard mass	Formula	Error (mDa)	Error (ppm)	Loss of group
AS−MG	**Parent ion**	249.08809	249.08808	$C_{12}H_{13}O_4N_2$	0.01	+0.06	-
	fragment ions	147.05642	147.05639	$C_8H_7ON_2$	0.04	+0.25	$2CH_2CO+H_2O$
		161.07207	161.07204	$C_9H_9ON_2$	0.04	+0.22	$CH_2CO+CO+H_2O$
		179.08262	179.0826	$C_9H_{11}O_2N_2$	0.02	+0.12	CH_2CO+CO
		189.06698[a]	189.06695	$C_{10}H_9O_2N_2$	0.03	+0.13	CH_2CO+H_2O
		207.07755 [a]	207.07752	$C_{10}H_{11}O_3N_2$	0.04	+0.17	CH_2CO
		213.06697 [a]	213.06695	$C_{12}H_9O_2N_2$	0.02	+0.10	$2H_2O$
		231.07755 [a]	231.07752	$C_{12}H_{11}O_3N_2$	0.03	+0.13	H_2O
Gly−MG	**Parent ion**	182.04591	182.04588	$C_8H_8O_4N$	0.02	+0.13	-
	fragment ion	123.03261	123.032577	$C_6H_5O_2N$	0.03	+0.27	CH_2COOH

[a] fragment ions also observed in a previous study[17].

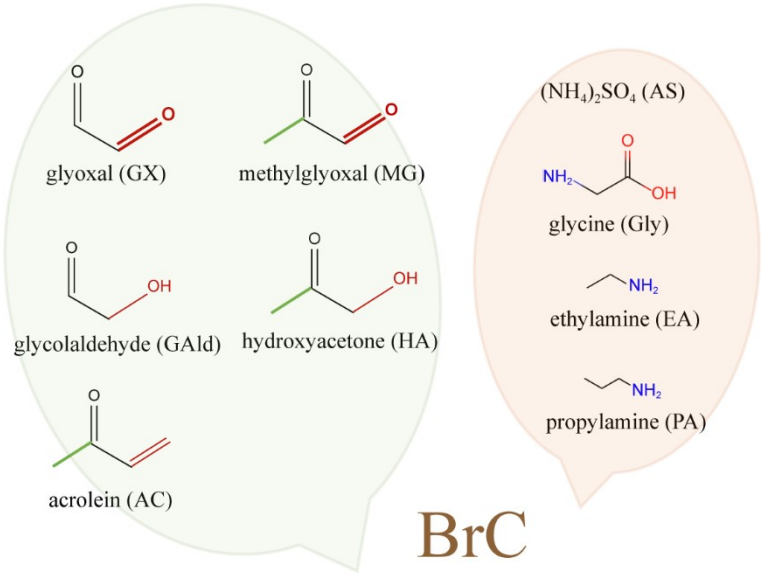

Scheme S1. Structuers of carbonyl compounds used in this study.

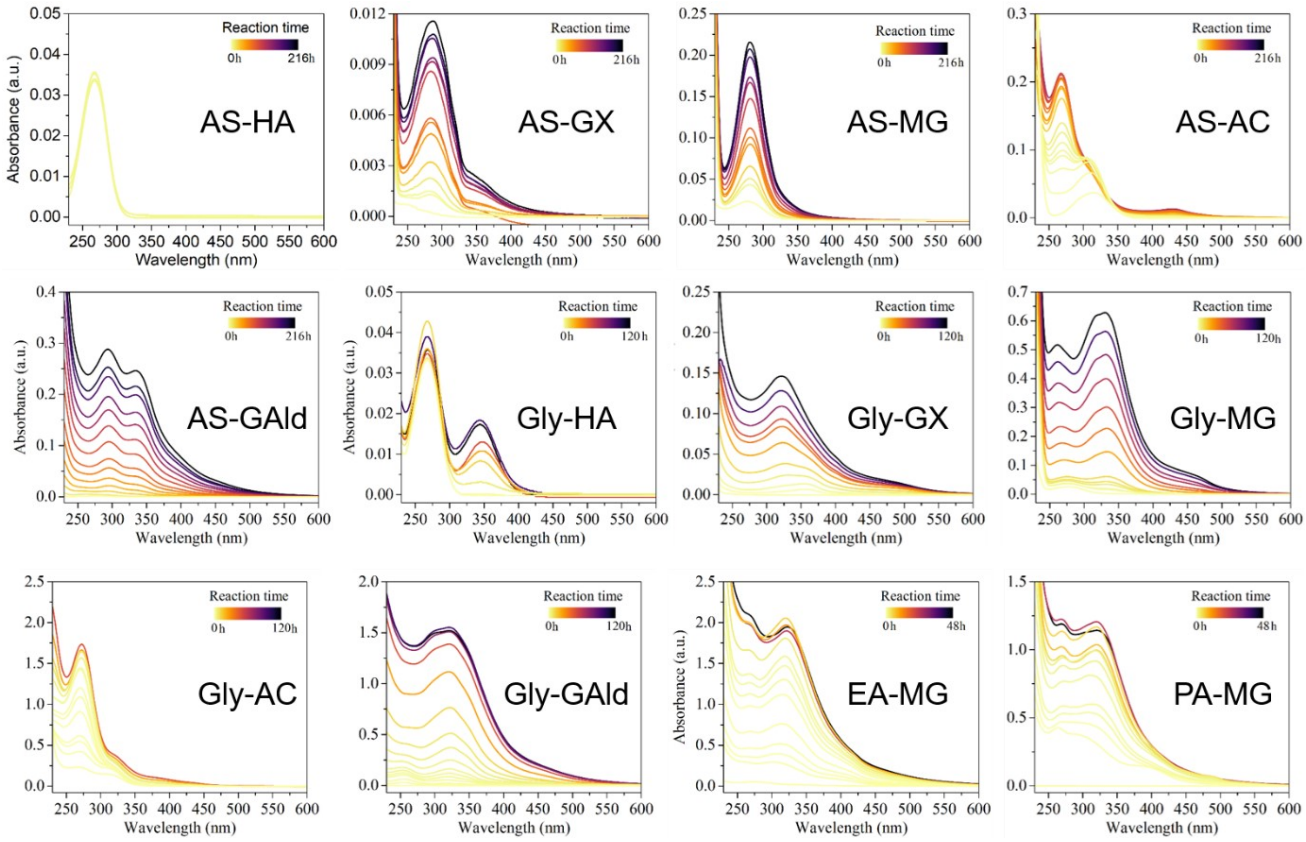

Fig. S1. Kinetic results for secondary brown carbon showing the change in the absorption as a function of time (AS: ammonium sulfate, HA: hydroxyacetone, GX: glyoxal, MG: methylglyoxal, AC: acrolein, GAld: glycolaldehyde, Gly: glycine, EA: ethylamine, PA: propylamine), all samples were diluted 300 times by ultrapure water before analysis.

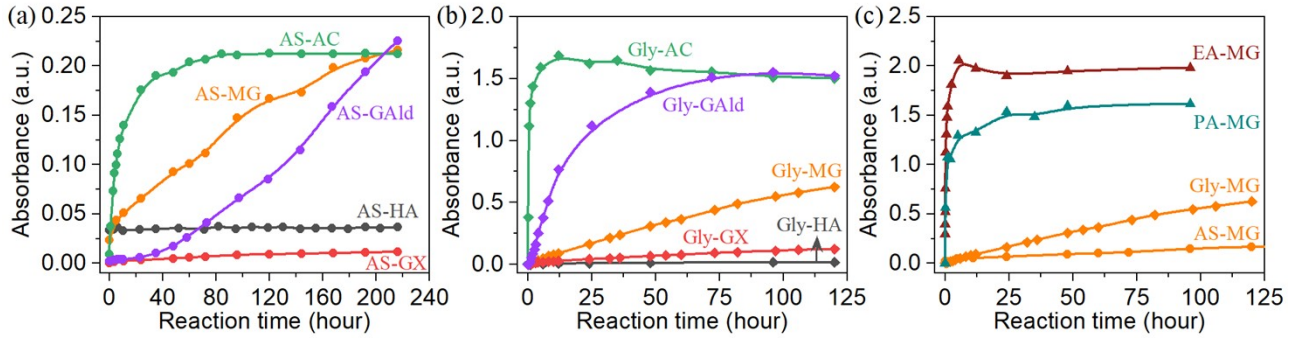

Fig. S2. Absorption changes of carbonyl compounds in AS (a) and Gly (b), and nitrogen-containing compounds in MG (c) as a function of time. The detection wavelengths are at λ = 267, 282, 281, 268, 290, 267, 331, 330, 272, 320, 320 and 315 nm for AS–HA, AS–GX, AS–MG, AS–AC, AS–GAld, Gly–HA, Gly–GX, Gly–MG, Gly–AC, Gly–GAld, EA–MG and PA–MG, respectively.

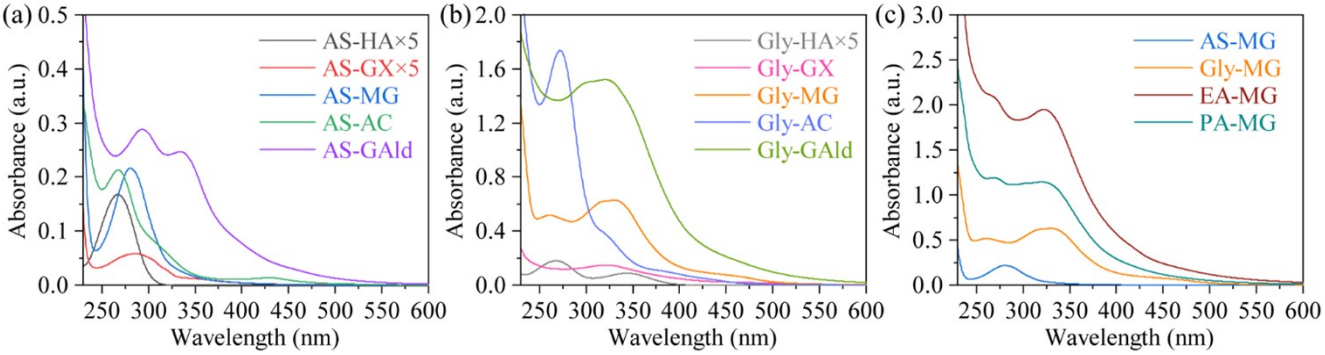

Fig. S3. UV–Vis spectra of 0.5 M carbonyl compounds in AS (a) and Gly (b), and nitrogen-containing compounds in MG (c); All samples were diluted by a factor of 300 before analysis and the spectra recorded after 2–9 d reaction time.

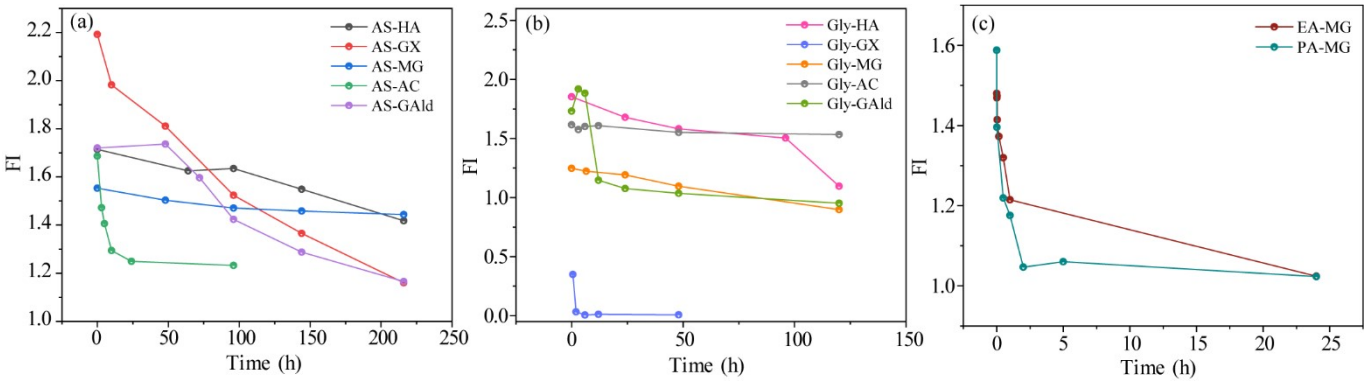

Fig. S4. Fluorescence index (FI) of carbonyl compounds in AS (a) and Gly (b), and nitrogen-containing compounds in MG (c) as a function of time.

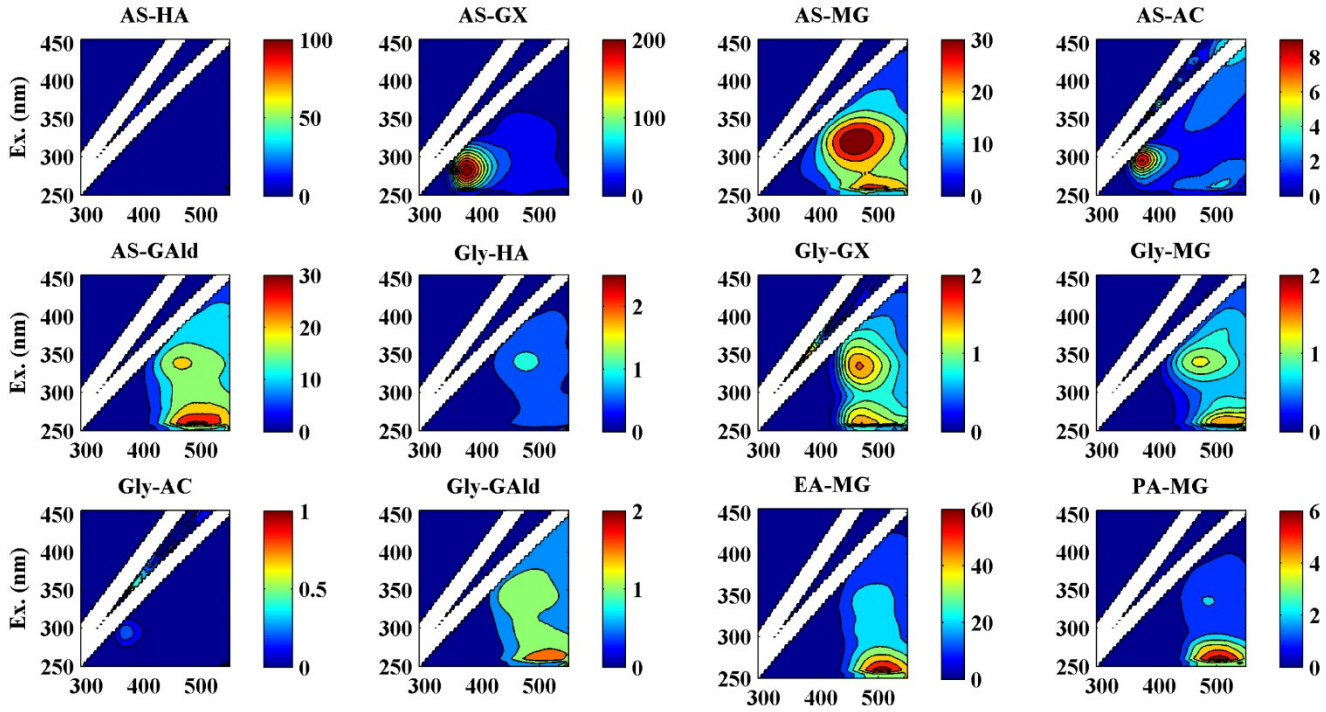

Fig. S5. The EEMs spectra for one set of secondary brown carbon products after solid-phase extraction (PPL). Note: The EEM region for secondary Rayleigh scatter was interpolated from either side of the scatter band after calibration.

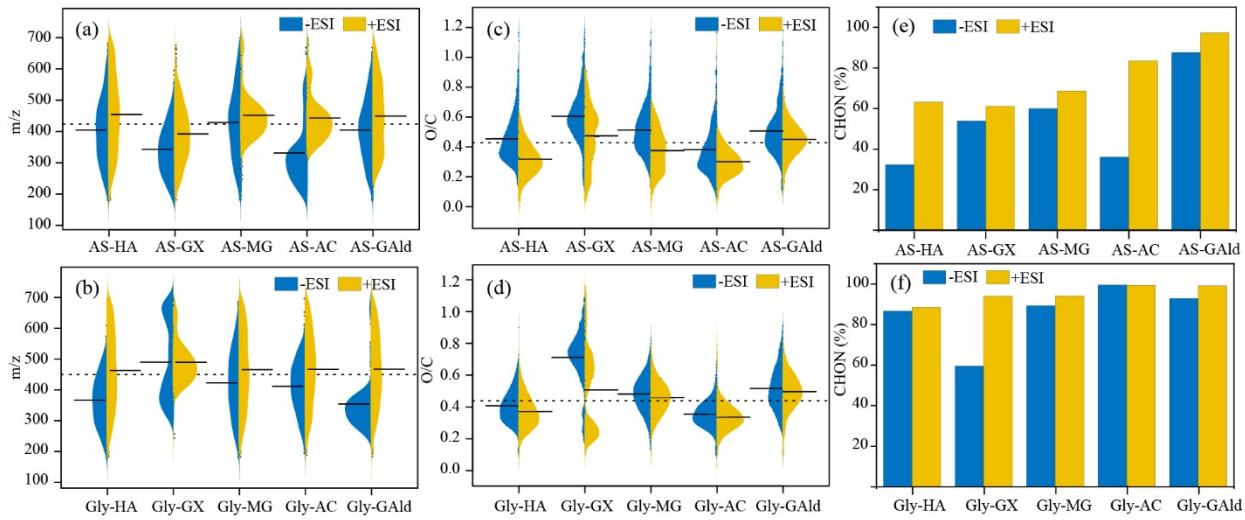

Fig. S6. Distribution of m/z values (a, b) and O/C values (c, d) were visualized using kernel-based cumulative density plots (violin plots). The black line of each band indicates the mean value. The percentages of CHON of each sample (e, f), blue represents the assigned formulas in –ESI, and yellow represents the assigned formulas in +ESI.

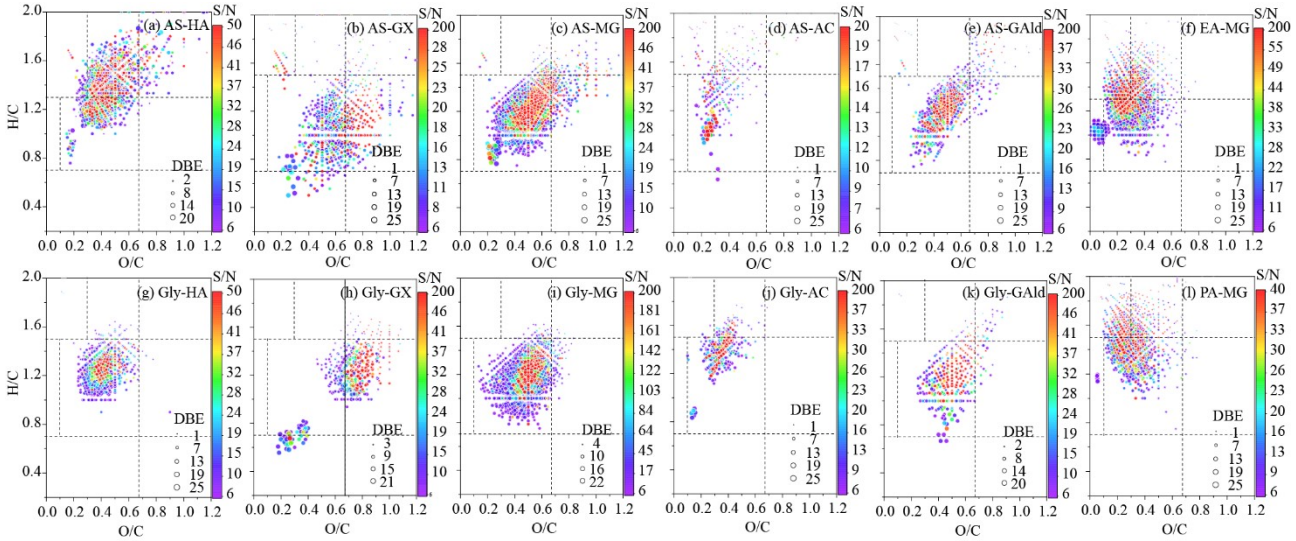

Fig. S7. Van Krevelen diagrams of the assigned formulas in –ESI for one set of secondary brown carbon products after solid-phase extraction. Color bars represent the signal-to-noise ratio (S/N) of peaks, and bubbles represent the double bond equivalence (DBE) values.

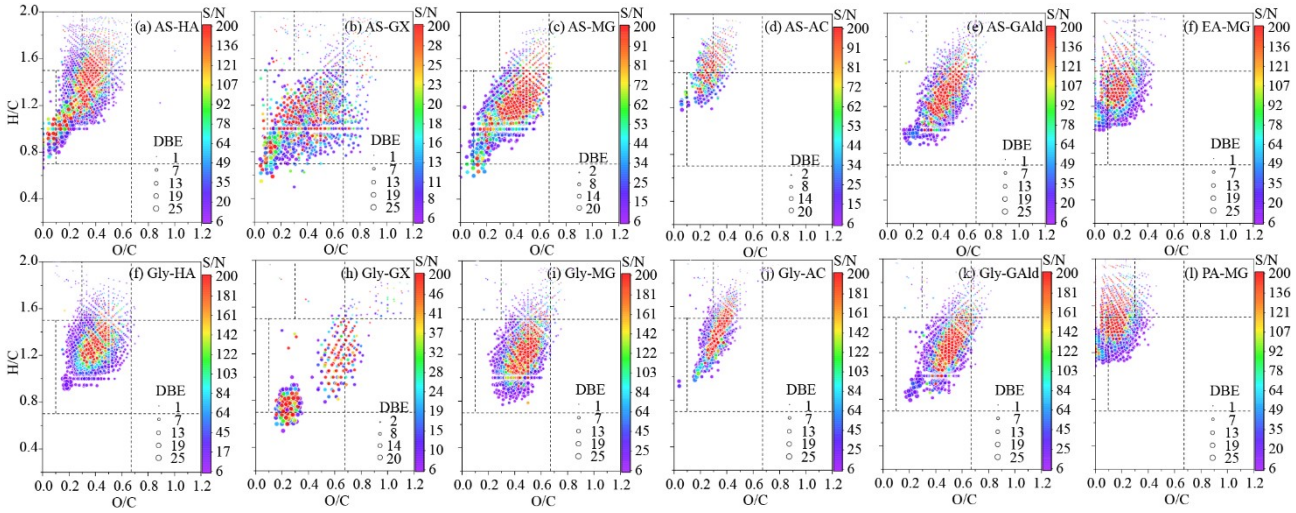

Fig. S8. Van Krevelen diagrams of the assigned formulas in +ESI for one set of secondary brown carbon products after solid-phase extraction. Color bars represent the signal-to-noise ratio (S/N) of peaks, and bubbles represent the double bond equivalence (DBE) values.

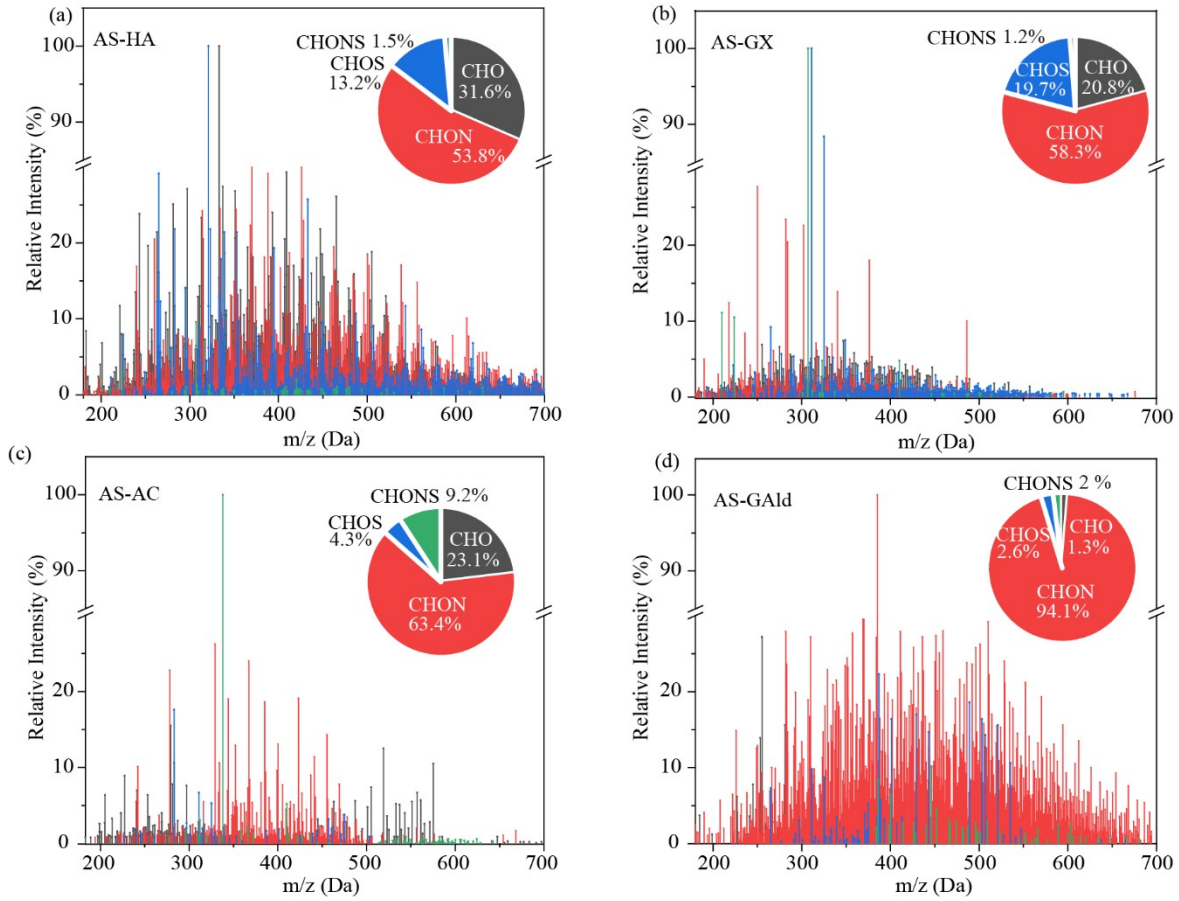

Fig. S9. ESI FT–ICR mass spectra of secondary brown carbon formed by the reaction of AS with HA (a), GX (b), AC (c) and GAld (d) combined –ESI and +ESI modes. Different formula groups were color-coded. The pie charts showed the relative intensities of different formula groups.

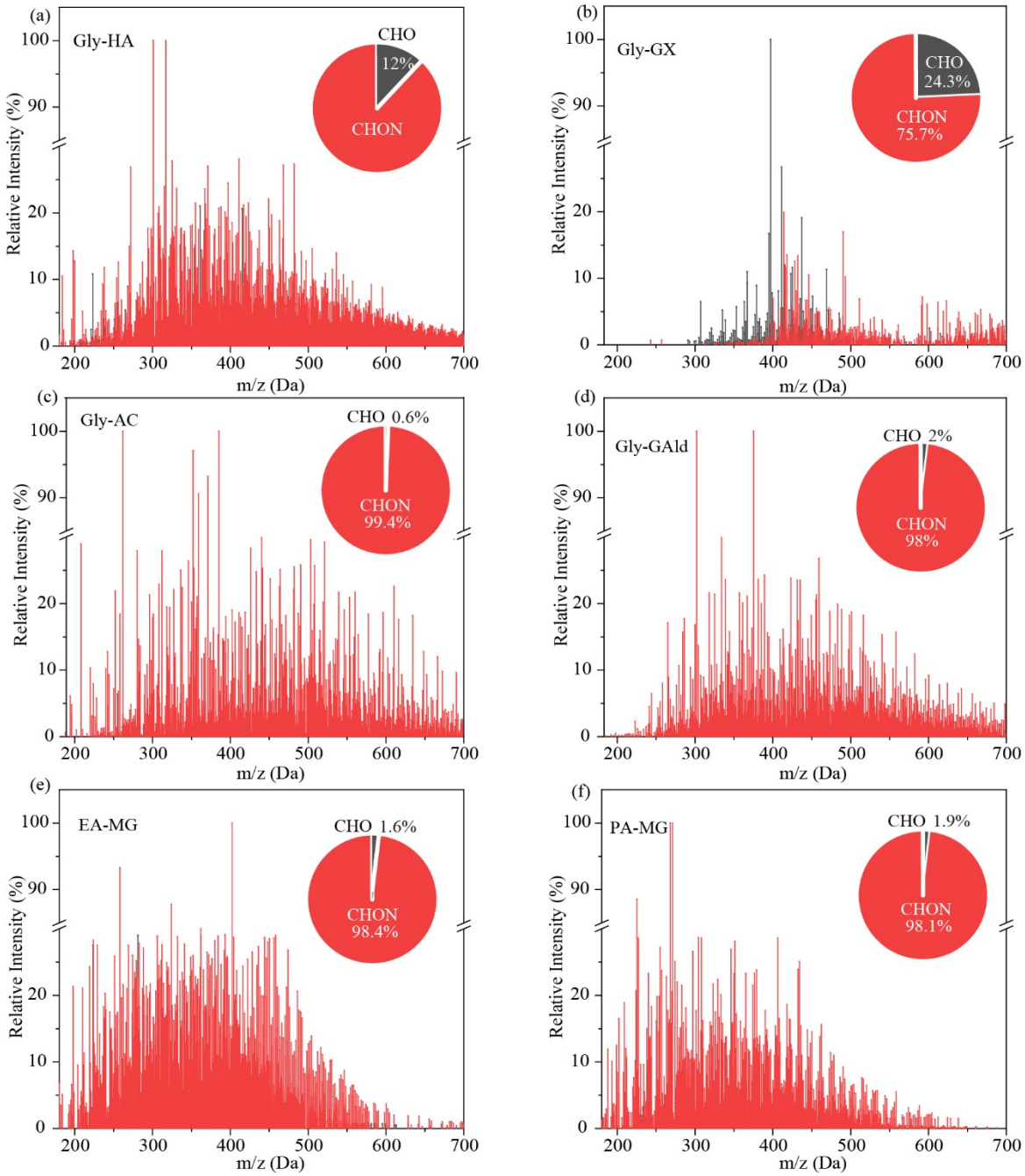

Fig. S10. ESI FT–ICR mass spectra of secondary brown carbon formed by the reaction of Gly with HA (a), GX (b), AC (c) and GAld (d), and the reaction of MG with EA (e) and PA (f) combined –ESI and +ESI modes. Different formula groups were color-coded. The pie charts showed the relative intensities of different formula groups.

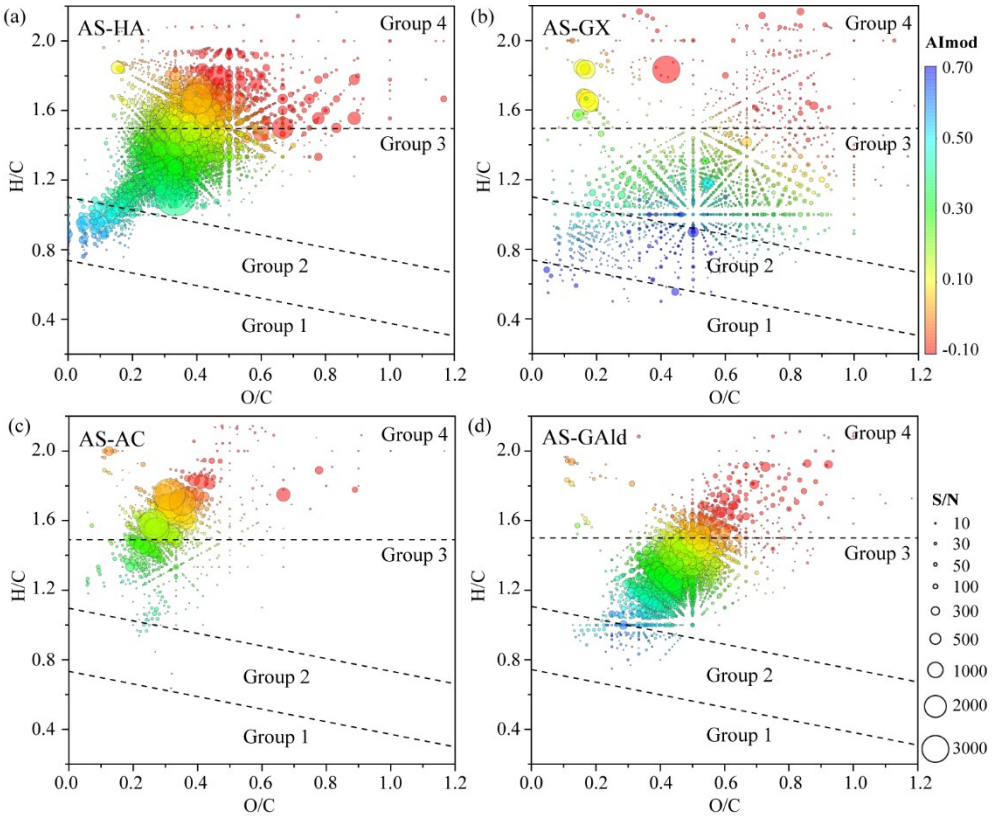

Fig. S11. Van Krevelen diagrams of identified formulas in BrC formed by AS, color bar represents the aromaticity index (AI_{mod}) and bubble size represents the signal-to-noise ratio (S/N); four groups in van Krevelen diagram are delineated by AI_{mod} and H/C cutoffs (Group 1: condensed polycyclic aromatics; Group 2: polyphenols; Group 3: highly unsaturated and phenolic compounds; Group 4: aliphatic compounds).

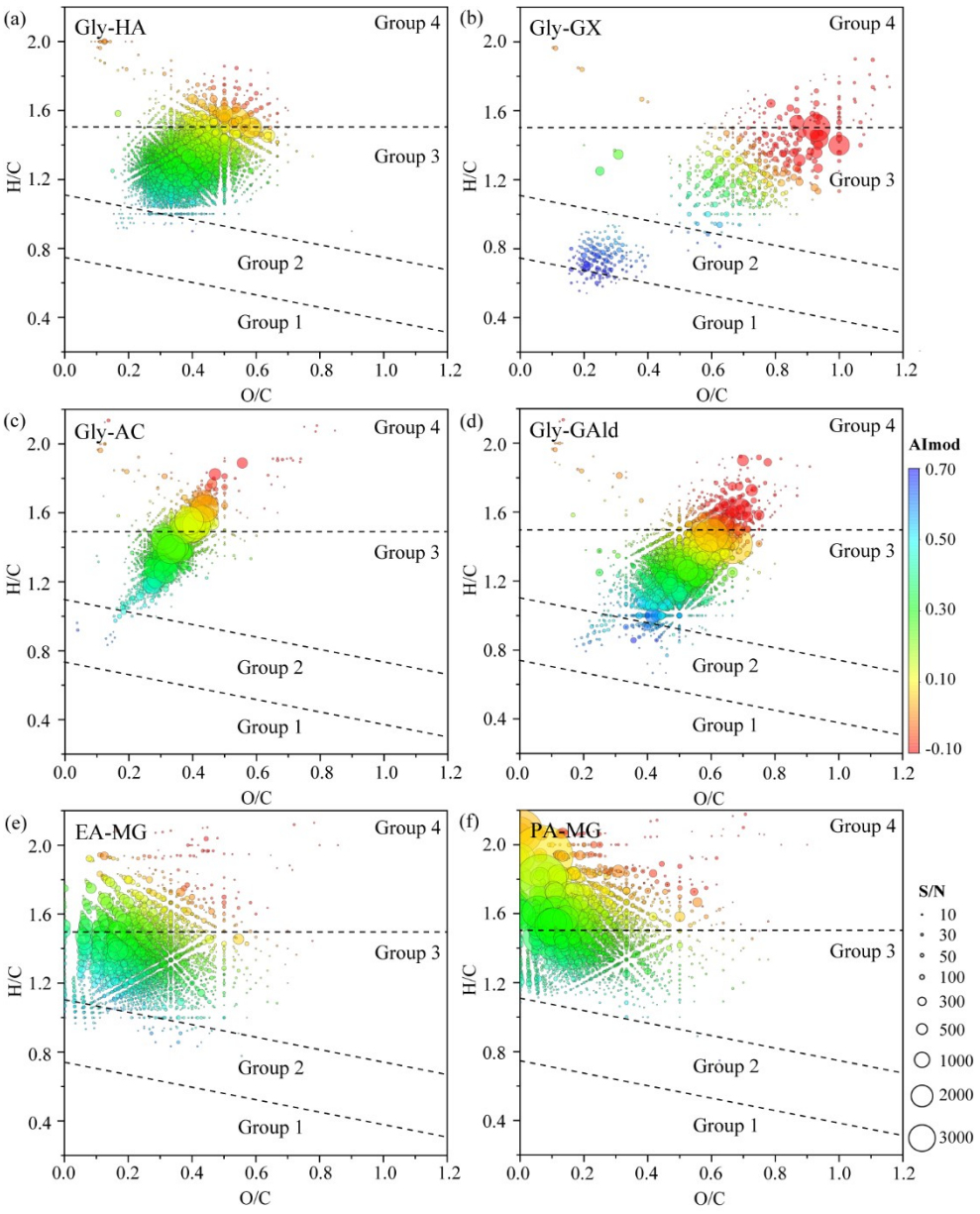

Fig. S12. Van Krevelen diagrams of identified formulas in BrC formed by Gly and MG, color bar represents the aromaticity index (AI_{mod}) and bubble size represents the signal-to-noise ratio (S/N); four groups in van Krevelen diagram are delineated by AI_{mod} and H/C cutoffs (Group 1: condensed polycyclic aromatics; Group 2: polyphenols; Group 3: highly unsaturated and phenolic compounds; Group 4: aliphatic compounds).

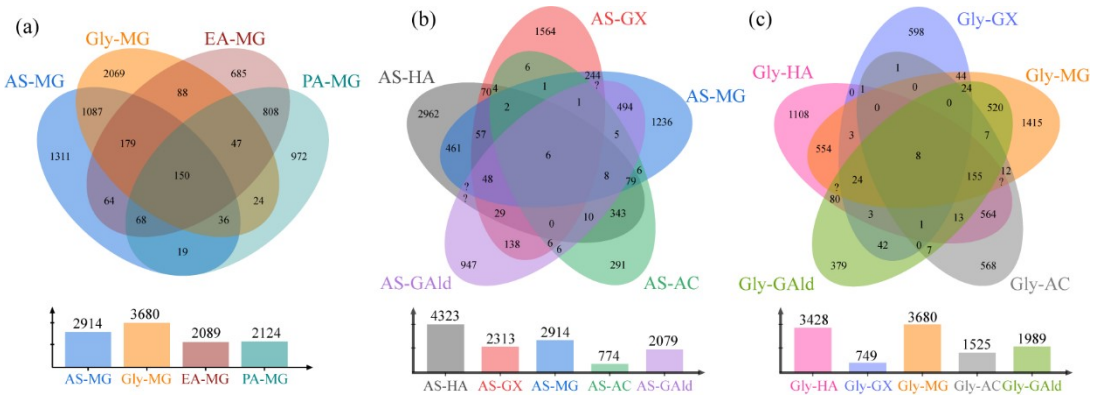

Fig. S13. Venn diagrams illustrating the number of the shared and unique formulas of secondary BrC studied here.

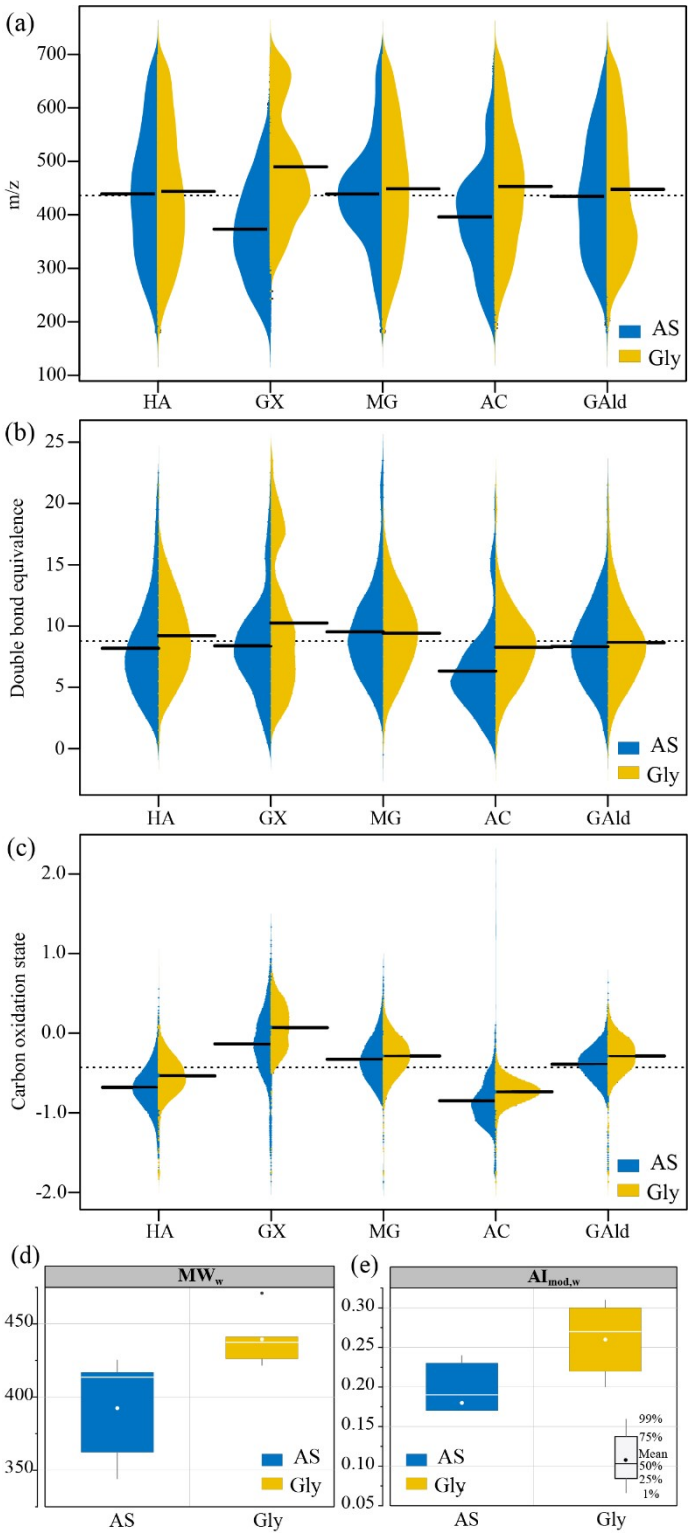

Fig. S14. Distribution of m/z values (a), double bond equivalence (b) and carbon oxidation state values (c) were visualized using kernel-based cumulative density plots (violin plots), left half represents the assigned formulas of BrC formed by AS, and right half represents the assigned formulas of BrC formed by Gly. The black line of each band indicates the mean value; values of magnitude molecular weight (MW_w) (d) and magnitude modified aromaticity index ($AI_{mod,w}$) (e).

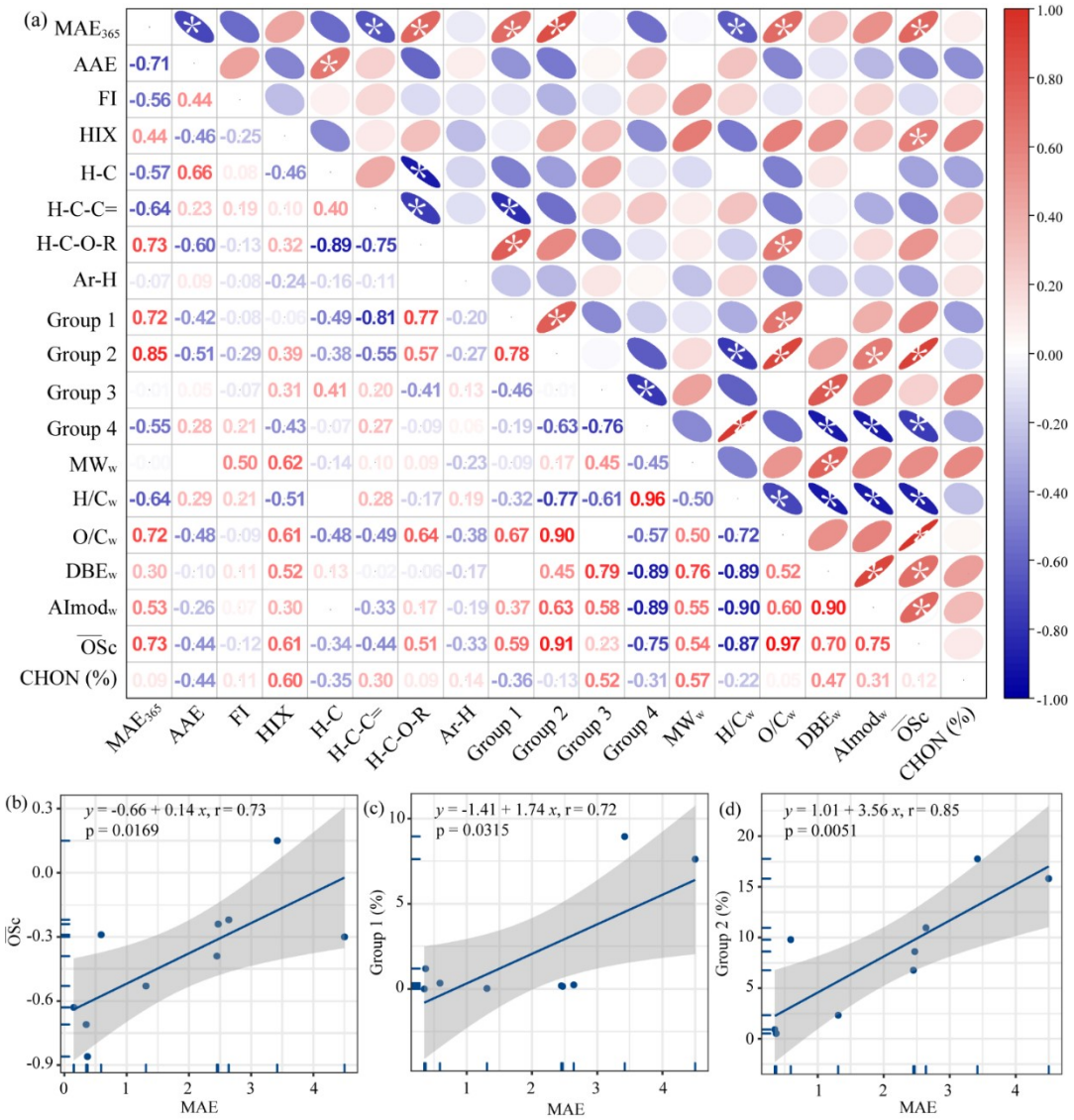

Fig. S15. Pearson correlation matrix of optical parameters with molecular characteristics and compositions for the assigned formulas. Colors from blue to red represent changes in the Pearson correlation coefficient from −1 to 1. The "*" represents significant correlation ($p \leq 0.05$).

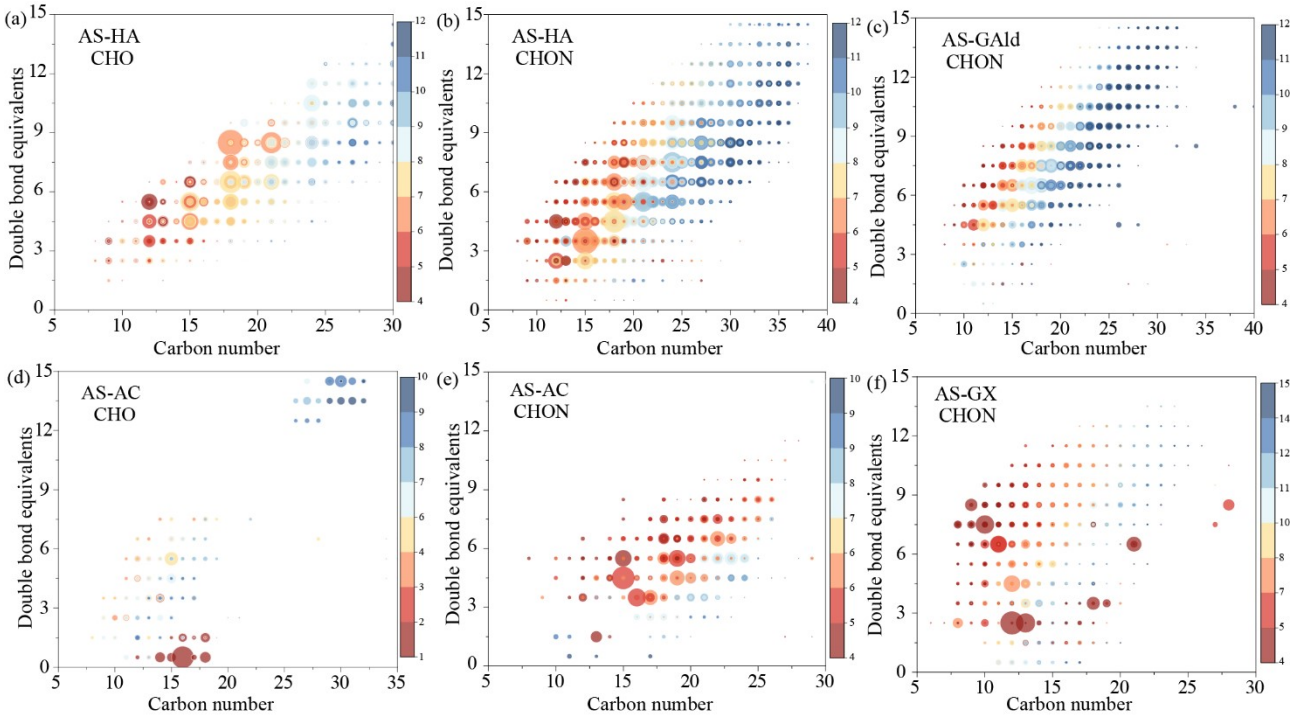

Fig. S16. DBE vs C number for the CHO and CHON compounds of BrC formed by AS with different carbonyl compounds. The color bar and marker size denote the number of O atoms and the peak intensities of the compounds.

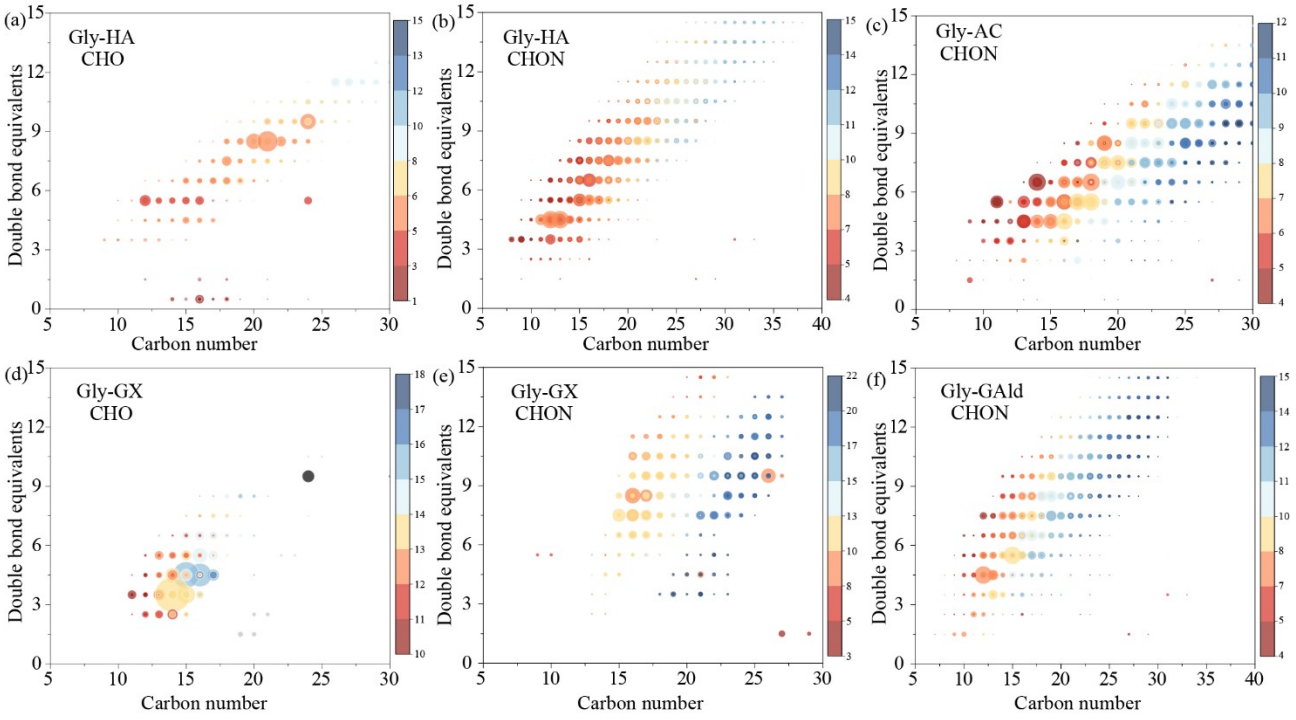

Fig. S17. DBE vs C number for the CHO and CHON compounds of BrC formed by Gly with different carbonyl compounds. The color bar and marker size denote the number of O atoms and the peak intensities of the compounds.

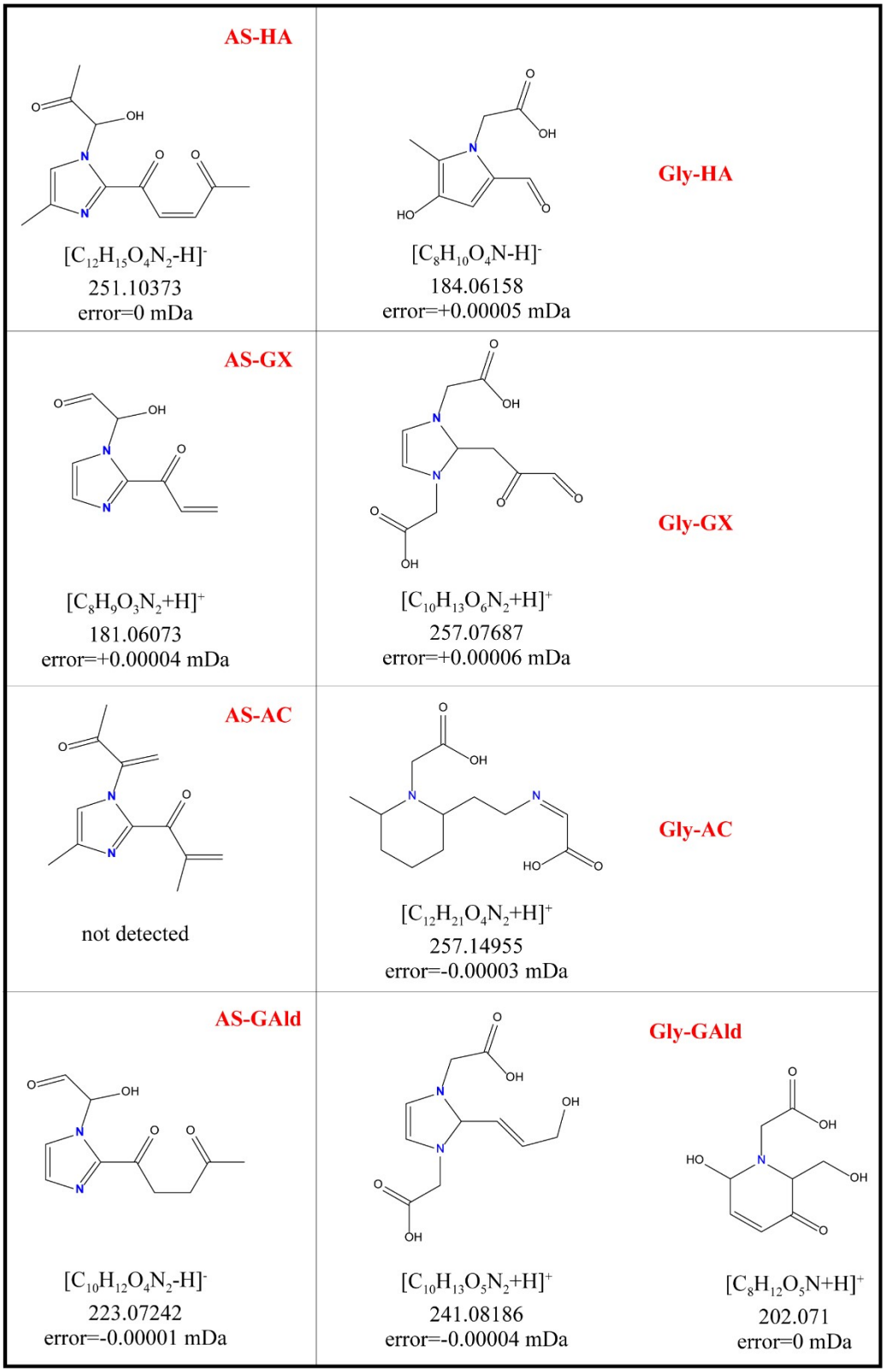

Fig. S18. Proposed molecular structures of secondary BrC samples in this study.

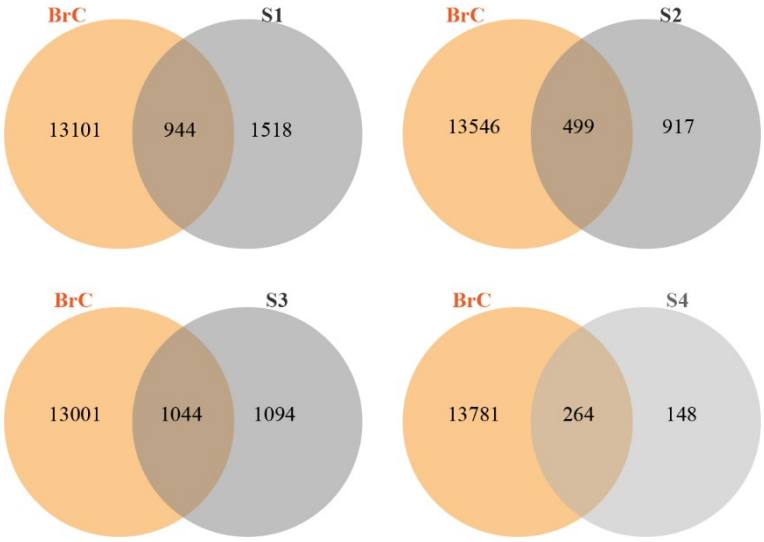

Fig. S19. Venn diagrams illustrating the number of the shared and unique formulas between secondary BrC and atmospheric samples.